

Distortion of the luminosity function of high-redshift galaxies by gravitational lensing

Anastasia Fialkov, Ecole Normale Supérieure, Paris, France
Abraham Loeb, Harvard University, Cambridge, USA
arXiv:1502.03141

We consider the effects of gravitational lensing on the luminosity function of Lyman-break galaxies (LBGs) at redshifts 6 – 15 and sub-mm galaxies (SMGs) at redshift 2.6, focusing on the lensing with intermediate magnifications $\mu \leq 2$.

Background

Detection of the high-redshift galaxies is a primary frontier in observational cosmology. Sampling and analyzing the properties of different types of high-redshift sources will constrain galaxy formation and star formation histories at different epochs, and explain their role in reionization and metal enrichment of the Universe. However, the observed properties of these galaxies depend on the underlying foreground distribution of large scale structure, which distorts their intrinsic properties via gravitational lensing. Because intrinsically bright background sources are rare objects, an observed bright source has an enhanced likelihood of being a magnified intrinsically fainter galaxy, which are much more abundant, thus leading to an overestimation of the intrinsically bright population and distorted appearance of its luminosity function. Strong lensing is relatively easy to spot, but it is rare with a raw probability for multiple images at the highest source redshifts of only 0.5% [1]. On the other hand, most of the galaxies are lensed with weak and intermediate magnifications (i.e., when no multiple images are produced, $\mu \leq 2$). In this case the effect of lensing can be easily overlooked leading to an over (or under) prediction of the number counts of background galaxies, and thus, to an erroneous estimation of their properties. The effect of the intermediate and small magnifications on the observed properties of high redshift sources, such as their luminosity function, has not been properly addressed in the literature and is considered here.

Model ingredients and basic steps:

- Foreground mass profile.** We use (i) **virialized halos** hosting bright galaxies, where three-dimensional density profile is modeled as a combination of NFW and singular isothermal sphere (SIS) profiles to better match observations; (ii) **proto-clusters**, i.e., non-virialized mildly non-linear overdensities modeled by objects at turn around, with density profiles being spherical top-hat.
- Spatial distribution of foreground lenses.** We use the Sheth & Tormen mass function.
- Sources.** We consider two types of high-redshift galaxies: (i) dusty galaxies at $z \sim 3$ observed in sub-mm range by ALMA (SMGs); (ii) redshift 6 - 15 galaxies observed via Lyman-break techniques by HST and JWST (LBGs).
- Redshift distribution of SMGs.** We use the distribution from [5].
- Reduced lensing probability for LBGs behind a bright lens.** We use a toy model for the SED of foreground galaxies and account for K-corrections.
- The lensing probability.** Find $P(\mu)$ by first calculating the fraction of the sky that is lensed with magnifications larger than μ [2].
- Intrinsic populations.** We assume that the shape of the intrinsic (unlensed) number counts has the form of a Schechter function in the case LBGs [3] and either Schechter or broken power-law for the SMGs [4] (fig. 1).
- Lensed luminosity function.** We apply the lensing probability to the intrinsic flux distribution to determine the net effect of lensing on the observed luminosity function (fig 2).

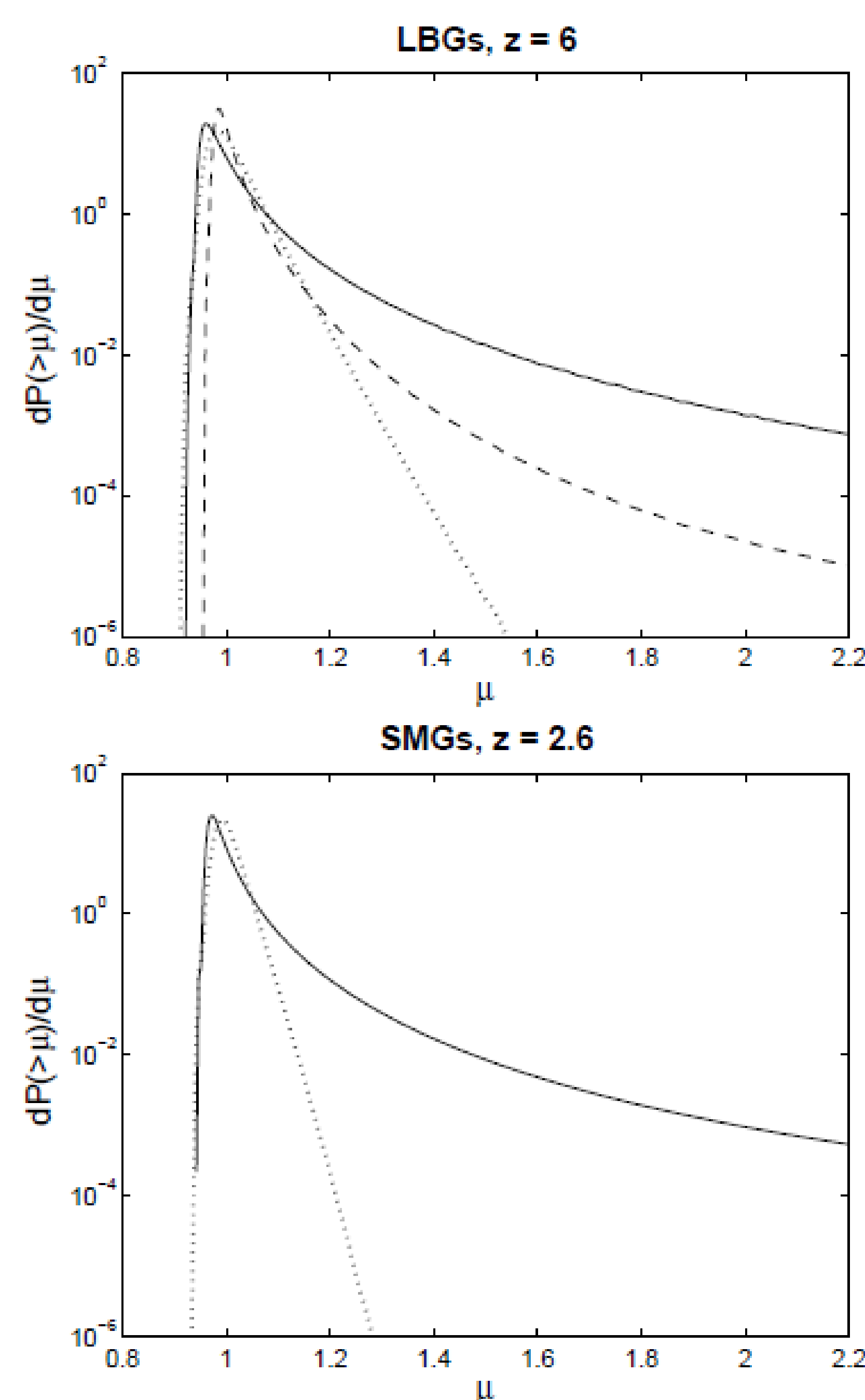


Figure 2: Probability distribution for lensing with magnification μ shown for a population of the Lyman-break galaxies (LBGs) at $z = 6$ (top) and of sub-mm (SMGs) galaxies at $z = 2.6$ (bottom). For SMGs, the lenses under consideration are virialized halos (solid) and proto-clusters (dotted). In the case of LBGs the sources are lensed by a population of virialized galaxies including the reduction in $P(\mu)$ (dashed) and ignoring it (solid), as well as by proto-clusters (dotted).

Reduced lensing probability for the LBGs behind a bright lens

LBGs located behind a bright extended lens can be observed if sufficiently magnified. Since foreground galaxies are normally bright in the observed bands which correspond to the rest frame UV bands of the sources, some images are too faint to be seen through the bright part of the lens even when they are magnified. The range of impact parameters (and thus magnifications) for which the high-redshift sources are observable is reduced when the constraints from surface brightness profiles are accounted for. This leads to a suppressed probability for obtaining intermediate and strong magnifications (fig. 2).

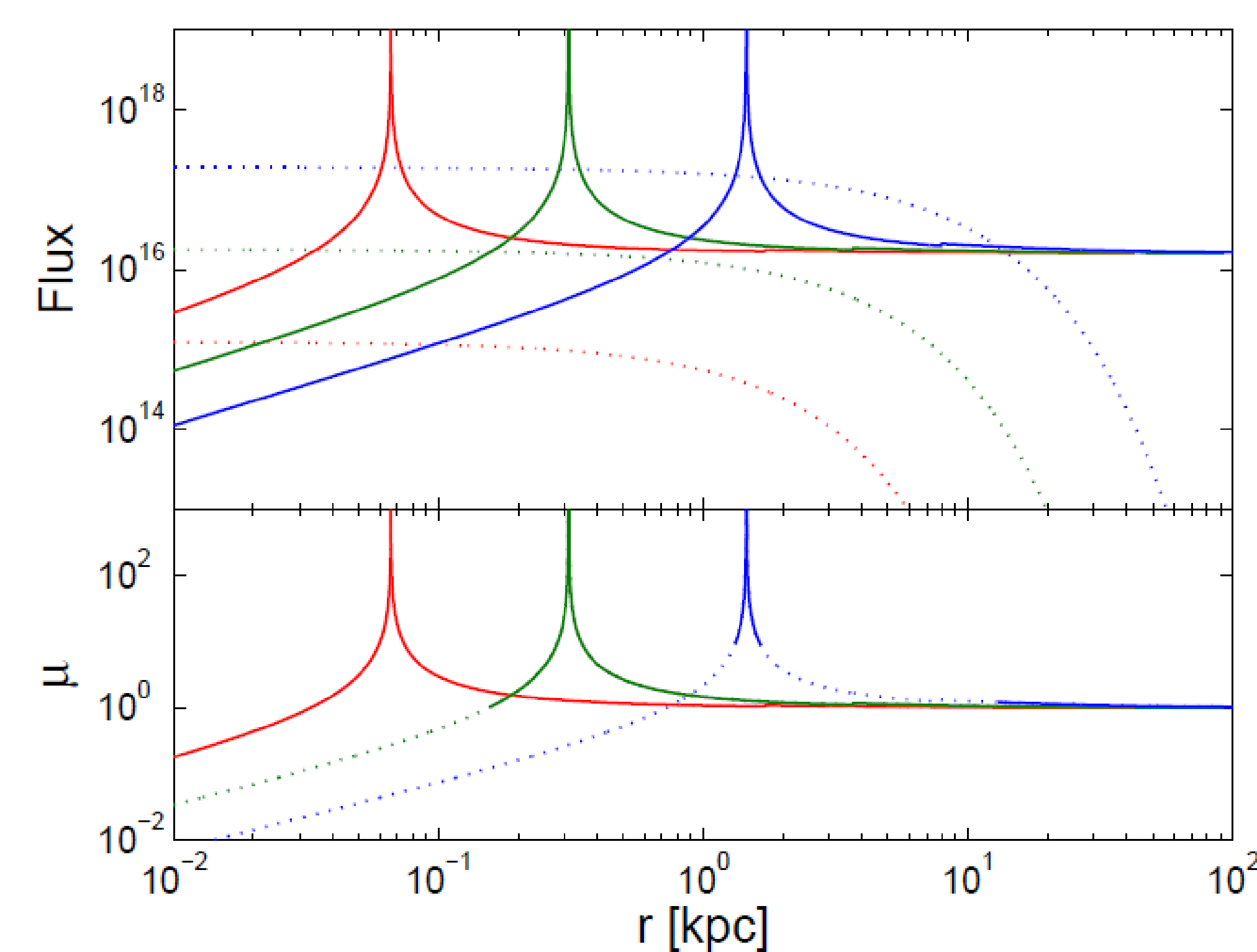


Figure 3: The top panels show the fluxes (in $\text{erg s}^{-1} \text{Hz}^{-1} \text{kpc}^{-2}$ units) of foreground galaxies (dotted lines) and the fluxes of a background galaxy magnified by each lens (solid lines) as a function of the physical impact parameter in the image plane. Source of mass $M = 10^{11} M_{\text{sun}}$ at redshift $z = 6$ are shown for three types of foreground galaxies at $z = 0.5$: $M = 10^{10} M_{\text{sun}}$ (red), $M = 10^{11} M_{\text{sun}}$ (green), and $M = 10^{12} M_{\text{sun}}$ (blue). The bottom panels show the corresponding magnification in each case in the observable part (solid lines) and non-observable part (dotted lines).

Results: Luminosity Function of High-redshift Field Galaxies

The observed luminosity function is affected by lensing and may have a completely different shape than the intrinsic one. Lensing has very little impact on the luminosity function in the faint-end, but it may have a strong impact on the number counts of high-luminosity sources.

Our main results are as follows:

- The effect of lensing on the parameters of the luminosity function of LBGs (fig. 4 and table 1) is not relevant for current surveys with Hubble Space Telescope.
- The effect of lensing on the parameters of the luminosity function of LBGs starts to manifest itself if the brightest observed sources have $M_{\text{UV}} \leq -22.5$. In this regime, by comparing the strong lensing case to the no-lensing case we get a $\sim 3\%$ discrepancy for LBGs at $z = 15$ in the value of the normalization of the number counts.
- In the case of LBGs it is important to consider surface brightness profiles of both the lens and the source. Unaccounted it may lead to two orders of magnitude discrepancy in the luminosity function at the bright end (fig. 4).
- The effect of proto-clusters is comparable to lensing by halos with $\mu < 1.4$ when the sources are LBGs.
- The effect of lensing on SMGs is highly unconstrained and may be very strong (fig. 5 and table 2).
- The effect of proto-clusters in the case of the SMGs it negligible even when compared to lensing by halos with $\mu = 1.3$.

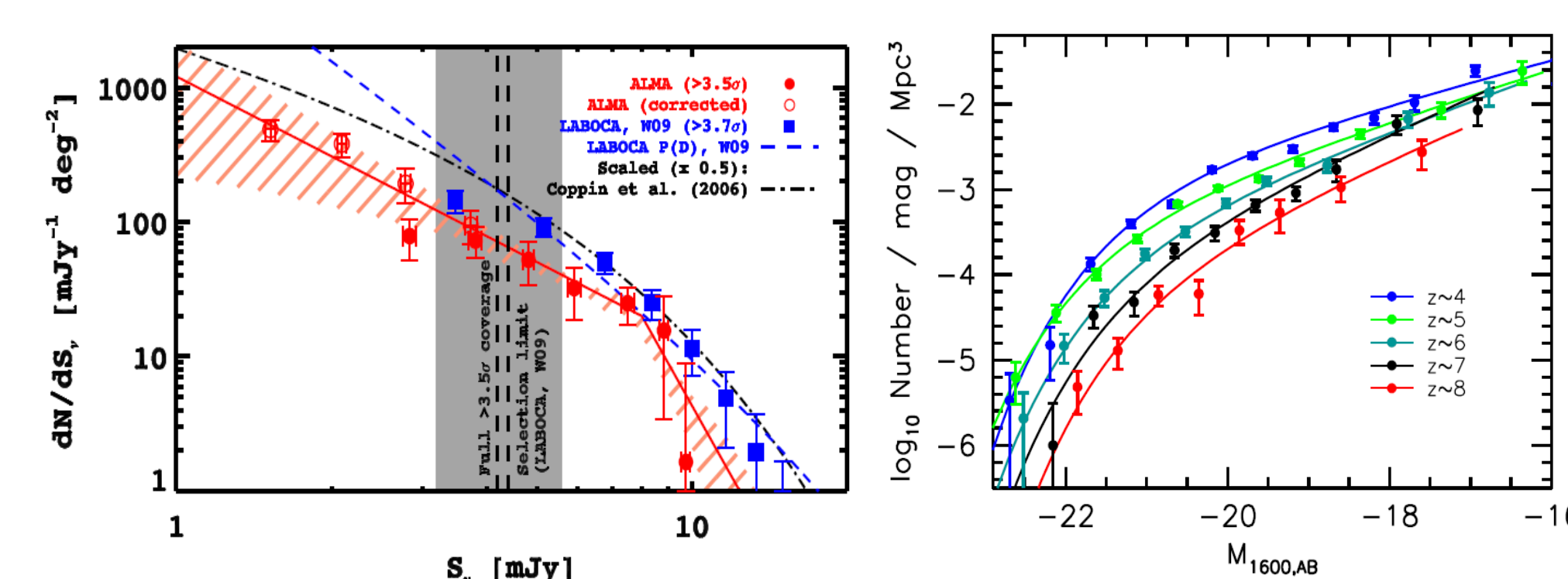


Figure 1: Observed number counts of sub-mm galaxies (left [4]) and Lyman-break galaxies (right [3]).

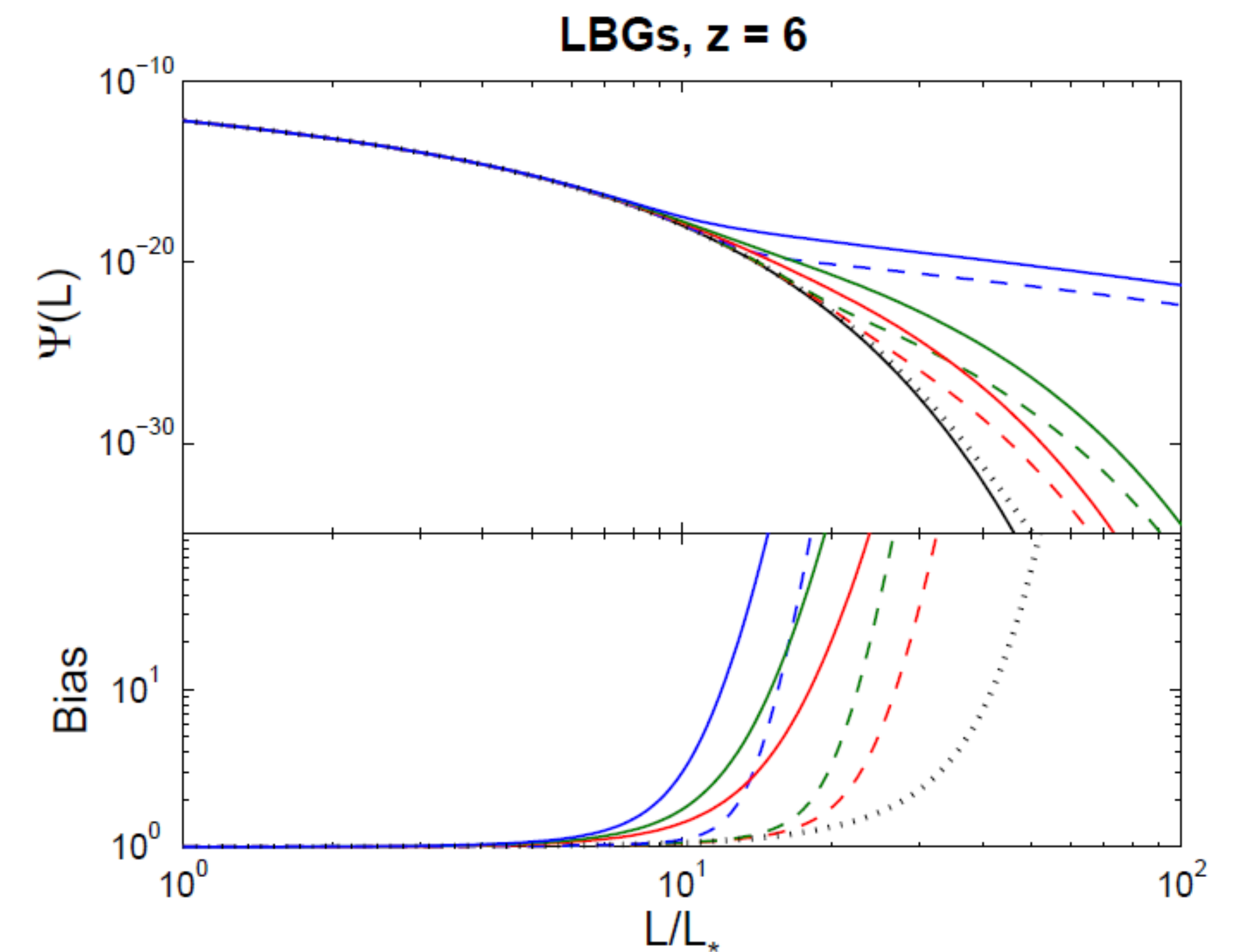


Figure 4: The luminosity function (top panels) and the magnification bias (bottom panels) of the LBGs at $z = 6$. We show the intrinsic luminosity function (black line), and the luminosity function of LBGs lensed by a population of virialized objects including the reduction in $P(\mu)$ for all possible magnifications (dashed) and ignoring it (solid) for magnifications $\mu \leq 2$ (red), $\mu \leq 3$ (green), $\mu \leq 1000$ (blue) as well as for LBGs lensed by non-virialized objects at turn around (black dotted).

Redshifts	$\mu_{\text{max}} = 1.3$	$\mu_{\text{max}} = 1.5$	$\mu_{\text{max}} = 1.7$	$\mu_{\text{max}} = 2$	$\mu_{\text{max}} = 3$	$\mu_{\text{alt}}^{\text{in}}$
6	1.7, 2.7%	2.4, 4.1%	3.6, 5.4%	7.2, 8.0%	64.5, 16.24%	1.7, 2.9%
8	2.0, 4.1%	3.5, 6.7%	6.4, 9.4%	15.7, 13.3%	188.1, 25.2%	2.3, 4.9%
10	2.4, 5.6%	5.0, 9.8%	10.8, 13.9%	32.9, 19.8%	484.2, 34.4%	3.1, 7.4%
12	2.8, 7.7%	7.1, 13.3%	18.4, 19.3%	64.6, 26.7%	$> 10^3$, 43.8%	4.3, 10.1%
15	3.6, 11.1%	12.0, 19.6%	37.1, 27.6%	166.4, 37.9%	$> 10^3$, 57.3%	7.4, 14.9%

Table 1: Summary of the errors introduced by gravitational lensing by virialized halos in the luminosity function of LBGs at different redshifts. Each entry contains the pair of values: (Bias, $\Delta\Psi\%$) introduced by lensing with $\mu < 1.3, 1.5, 1.7, 2$ and 3 in the parameters of the Schechter luminosity function. In addition, we show the case of the lensing by proto-clusters with all possible magnification (the last column). Fits are done for the luminosities in the range of magnitudes larger than the detection limit of HST (for sources at $z \leq 10$) and JWST (for $z > 10$) and for the bright magnitude limit $MUV = -24.5$.

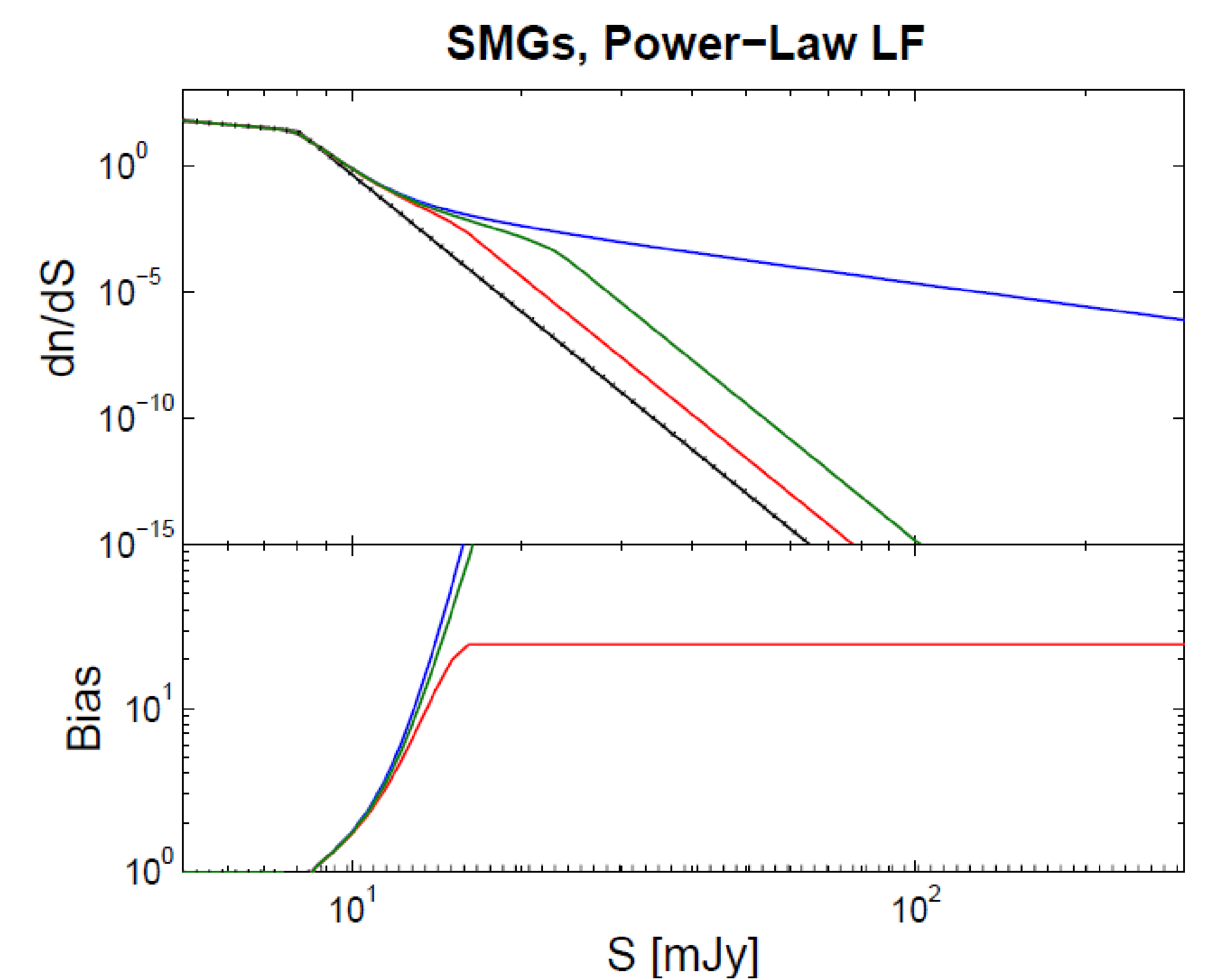


Figure 5: The luminosity function (top panels) and the magnification bias (bottom panels) of the SMGs. We show the intrinsic luminosity function (black line), and the luminosity functions lensed by a population of virialized objects for magnifications $\mu \leq 2$ (red), $\mu \leq 3$ (green), $\mu \leq 1000$ (blue) as well as by proto-clusters (black dotted).

Model	$\mu_{\text{max}} = 1.3$	$\mu_{\text{max}} = 1.7$	$\mu_{\text{max}} = 2$	$\mu_{\text{max}} = 3$	$\mu_{\text{alt}}^{\text{in}}$
Flat	2.3, 3.8%, 2.1%	13.6, 10.5%, 6.2%	44.1, 14.7%, 9.4%	518.8, 23.8%, 17.5%	1.1, 0.5%, 0.2%
Best fit	2.6, 7.7%, 2.6%	20.1, 20.4%, 8.3%	77.1, 28.5%, 12.5%	$> 10^3$, 44.4%, 22.8%	1.1, 1.1%, 0.4%
Steep	2.9, 10.9%, 3.0%	27.9, 28.8%, 9.6%	122.6, 39.7%, 15.1%	$> 10^3$, 59.5%, 30.0%	1.2, 1.7%, 0.5%

Table 2: Summary of the errors introduced by gravitational lensing in the luminosity function of SMGs at $z = 2.6$. Each entry contains the values of (Bias, $\Delta N\%$, $\Delta S\%$) introduced by lensing due to virialized halos with $\mu \leq 1.3, 1.5, 1.7, 2$ and 3 , as well as proto-clusters in the parameters of the Schechter luminosity function. The fits are done for the luminosities in the range $3 \text{ mJy} < S < 25 S^*$ and the values of bias are quoted at $S = 25 S^*$.

References:

- [1] Barkana, R., and Loeb, A., 2000, *ApJ*, **531**, 613; Comerford, J. M., Haiman, Z., and Schaye, J., 2002, *ApJ*, **580**, 63
- [2] Lima, M., Jain, B., and Devlin, M., 2010, *MNRAS*, **406**, 2352; Wardlow, J., L., Cooray, A., De Bernardis, F., Amblard, A., Arumugam, V., 2013, *ApJ*, **762**, 59
- [3] Bouwens, R. J., et al., 2014, arXiv:1403.4295
- [4] Karim, A., et al., 2013, *MNRAS*, **432**, 2
- [5] Simpson, J. M., et al., 2014, *ApJ*, **788**, 125